Title
Access of ligands to cavities within the core of a protein is rapid

Journal
Nature Structural & Molecular Biology, 3(6)

ISSN
1545-9993

Authors
Feher, Victoria A
Baldwin, Enoch P
Dahlquist, Frederick W

Publication Date
1996-06-01

DOI
10.1038/nsb0696-516

Peer reviewed

Access of ligands to cavities within the core of a protein is rapid

Victoria A. Feher, Enoch P. Baldwin and Frederick W. Dahlquist

We have investigated the magnitude and timescale of fluctuations within the core of a protein using the exchange kinetics of indole and benzene binding to engineered hydrophobic cavities in T4 lysozyme. The crystal structures of variant–benzene complexes suggest that relatively large scale fluctuations (1–2 Å) of backbone atoms are required for entry of these ligands into the core. Nonetheless, these ligands enter the cavities rapidly, with bimolecular rate constants of ~10^6–10^7 M^{-1} s^{-1} and a low activation barrier, 2–5 kcal mol^{-1}. These results suggest that protein cores undergo substantial fluctuations on the millisecond to microsecond timescale and that entry of small molecules into protein interiors is not strongly limited by steric occlusion.

Institute of Molecular Biology and Department of Chemistry, University of Oregon, Eugene, Oregon 97403, USA

Correspondence should be addressed to F.W.D.

Knowledge of the types, magnitudes, and frequencies of dynamic fluctuations available to proteins is important in defining the molecular details and rate-limiting processes of protein functions such as ligand binding, protein–protein interactions, and conformational changes[1–4]. Currently, X-ray crystallography and NMR spectroscopy depict the time-averaged structures of proteins with well ordered and relatively static interiors but with more flexibility of surface regions. Crystallographic *B*-factors and the root-mean-square (r.m.s.) deviations for an NMR ensemble of structures indicate buried atoms have small deviations from their mean position (0.25–0.5 Å), while surface residue deviations can be much larger, up to several angstroms[5,6]. Neutron scattering, molecular dynamic simulations, and NMR relaxation studies have assigned picosecond timescales to the small motions of buried side chains[7–11]. Larger scale rapid fluctuations are revealed by buried aromatic rings that flip faster than 10^4 s^{-1} (refs 12, 13). Concerted fluctuations up to 3 Å occur on the millisecond to microsecond timescale and are limited to surface accessible residues, loops, active site residues, and the terminal ends of proteins[4,11]. Ligand exchange kinetics have also been utilized to probe the fluctuations available to protein cores. These studies are consistent with the small scale motions of core atoms on the picosecond timescale since monoatomic and diatomic molecules and solvent can rapidly access the buried regions of proteins[14–21]. Are larger scale fluctuations available to protein cores? To answer this question we have used NMR to measure how fast larger molecules, benzene and indole (Fig. 1), enter and exit from engineered internal cavities in T4 lysozyme variants.

Benzene-binding variants of T4 lysozyme

Benzene stabilizes two T4 lysozyme variants by binding in the hydrophobic cavities created by mutations Leu99Ala and Met102Ala (refs 22, 23, E.P.B. *et al.*, unpublished results). The variant Leu99Ala also binds substituted benzenes, indole, and other 6,5 bicyclic compounds[24,25]. Crystal structures of the variant–ligand complexes show single ligand molecules bound in the solvent-inaccessible engineered cavities 5–6 Å from the surface (Figs 2*a–c*; refs 23, 25, E.P.B. *et al.*, unpublished results). In general, very little structural rearrangement occurs upon binding. However, in order for benzene to enter the cavities the conformation of the protein must alter significantly, suggesting that the primary barriers to entry and exit from the interior are the conformational changes required to create a free path. The entry rates of these ligands into interior cavities should represent a minimum estimate of the rate required for structural fluctuations. We investigated the rates of these fluctuations by measuring the exchange kinetics of benzene binding to T4 lysozyme variants Leu99Ala (Fig. 2*a*) and Met102Ala (Fig. 2*b*) under equilibrium conditions. The magnitude of these fluctuations was probed by comparing benzene rates with those of the larger indole molecule in the Leu99Ala variant (Fig. 1). Additionally, we compared the exchange kinetics of the cavity-containing variants to those of variant Phe104Ala (Fig. 2*c*), which binds benzene in a solvent accessible crevice. The entry rate constants for this variant should reflect the diffusional barrier for locating a benzene-sized binding site on the protein surface.

Binding and exchange kinetics by NMR

We determined binding occupancy and exchange rate constants as a function of benzene concentration by

following changes in the protein spectra. The variants were biosynthetically labelled with ^{15}N-alanine to provide easily identified resonances at the alanine-substituted binding site and several other positions (Fig. 3*a*). One-dimensional ^{15}N-edited ^{1}H NMR spectra of the alanine amides were obtained and the resonances were assigned using the published wild-type assignments, and data from two-dimensional ^{1}H,^{15}N-HSMQC, HSMQC-COSY and HSMQC-NOESY experiments. Representative spectra for the Leu99Ala variant are shown in Fig. 3*a*. The alanine amide resonances were divided into three groups, according to their responses to benzene binding: Type 1 did not change; Type 2 had moderate shifts (25–90 Hz) and little change in spectral linewidth, where the observed shift is the weighted average of the free and bound values; and Type 3 had large shifts (>100 Hz) and substantial line broadening, indicating an exchange contribution to the lineshape and position. Not surprisingly, the most perturbed resonances correspond to amides near the respective benzene binding sites (Fig. 3*a*). In contrast, the spectra of the wild-type protein were unaffected by saturating benzene concentrations (data not shown).

The chemical shirf changes of Type 2 amides were used to calculate the dissociation constants asuming a two state equilibrium (Fig. 3*b*). All three proteins bind benzene with similar affinity, ~10^{-3} M (Table 1), which is slightly higher affinity than expected from the partitioning of benzene between organic and aqueous phases (the partition coefficient for benzene transfer from octanol to aqueous phases is 7.4×10^{-3} (ref. 26)). These values correspond well to those obtained by monitoring the benzene concentration dependence of the folding/unfolding equilibrium[23] or by mixing calorimetry[24].

Table 1 Equilibrium dissociation constants and rate constants for benzene and indole binding to T4 lysozyme variants

a[1]		Leu99Ala	Met102Ala	Phe104Ala
K_d (mM),	10 °C	0.3 ± 0.20	0.4 ± 0.07	1.0 ± 0.11*
	20 °C	0.8 ± 0.12	0.8 ± 0.10	1.3 ± 0.05
	30 °C	1.1 ± 0.11	1.0 ± 0.08	N.D.[4]
k_{off} (s^{-1}),	10 °C	250 ± 50	3000 ± 800	>10^4*
	20 °C	800 ± 200	3000 ± 800	>10^4
	30 °C	950 ± 200	3000 ± 800	N.D.

b[2]	Indole	Benzene
K_d (mM):	0.35 ± 0.06	0.8 ± 0.12
k_{off} (s^{-1}):	325 ± 75	800 ± 200

c[3]	Variant + Benzene			Variant + Indole
	Leu99Ala	Met102Ala	Phe104Ala	Leu99Ala
k_{on} ($M^{-1}s^{-1}$)	8×10^5–1×10^6	3×10^6–5×10^6	>10^7*	7×10^5–1×10^6

[1]Dissociation constants and off rate constants for benzene to cavity and crevice containing T4 lysozyme mutants. Errors for dissociation constants are reported as the standard deviation from the mean value determined for several resonances, except for Phe104Ala at 10 °C where the goodness of fit is reported. Error estimates for the dissociation rate constants were determined from the range of simulations compared to the observed lineshape.
[2]Comparison of dissociation constant and off rate constant measured for indole and benzene binding to variant Leu99Ala at 20 °C.
[3]Values of bimolecular on rate constants evaluated using the relationship $k_{on}=K_d/k_{off}$.
[4]N.D.=not determined.
*The low temperature titration of benzene binding to Phe104Ala was done at 7 °C.

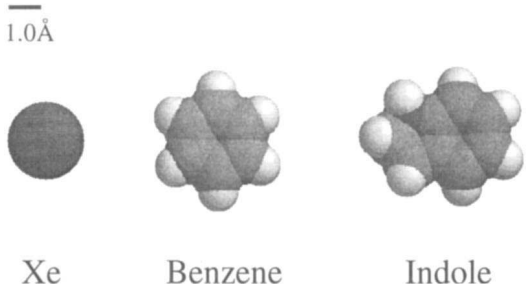

Fig. 1 Diagram of van der Waal size of xenon, benzene, and indole (ChemDraw3D, Cambridge Scientific Computing, Inc., Cambridge, MA.).

Analysis of the lineshapes of Type 3 resonances from titrations of Leu99Ala and Met102Ala yielded estimates of exchange rate constants, k_{ex} (see Ala 98, Fig. 3*a*). At equilibrium, k_{ex} is related to the dissociation rate constant, k_{off}, and the fraction bound, f_b, by $k_{ex}=k_{off}/f_b$. The k_{off} values were obtained from simulation of the lineshapes determined at several ligand concentrations, using relationships derived by McConnell[27] (Fig. 3*c*). The dissociation rate constants were 900 s^{-1} for Leu99Ala and 3000 s^{-1} for Met102Ala at 20 °C respectively (Table 1). The protein remains folded during the exchange process, the k_{off} values are much larger than the global unfolding rate constant which is on the order of weeks^{-1} (see Methods). Furthermore, benzene can bind directly to intact T4 lysozyme crystals[23], indicating that the fluctuations which allow benzene to bind in the cavity occur in the native state or a closely related state.

In contrast to the cavity-containing variants, the linewidths for resonances of the solvent accessible crevice-containing variant, Phe104Ala, remained narrow (data not shown). This lack of line-broadening indicates the ligand exchanges more rapidly than in Leu99Ala and Met102Ala, corresponding to k_{off} of 10,000 s^{-1} or more (see Methods). Thus, benzene escapes from the crevice faster than from the cavities.

Rapid entry to the protein core

Using the rate and equilibrium constants for dissociation, the apparent bimolecular rate constants for entry into the binding sites, k_{on}, were calculated: $k_{on}=k_{off}/K_d$ (Table 1). This analysis yielded k_{on} values of 1×10^6 M^{-1} s^{-1} and 4×10^6 M^{-1} s^{-1} for Leu99Ala and Met102Ala respectively. These values are within two to three orders of magnitude of the diffusion-controlled limit—the bimolecular diffusion controlled encounter rate constant, k_{on}, for a protein and a small molecule has been calculated to be ~10^9 M^{-1} s^{-1} (ref. 28) and rate constants measured for many enzymes and their substrates are in the 10^6–10^8 M^{-1} s^{-1} range[29]. The Met102Ala cavity is somewhat closer to the surface which may account for the fourfold faster rate of entry. The entry of benzene into the solvent accessible crevice of Phe104Ala is at least 10-fold faster, approaching the rate of diffusion.

We used the larger molecule, indole (10×6×4 Å, Fig. 1), to probe the magnitude of the necessary fluctuations for entry. Indole binds more tightly to Leu99Ala than benzene (K_d=3.5×10^{-4} M), and this is reflected by its slower rate of dissociation, k_{off}=325 s^{-1}. In the crystal structure of the Leu99Ala–indole complex, the indole Nε1 atom makes a hydrogen bond to the Sδ atom of Met 102 (ref. 25). Breakage of this bond upon dissociation may account for the slower off rate. In spite of its larger size, the k_{on} is essentially the same as for benzene (1×10^6 M^{-1} s^{-1}), suggesting the deformations that may be required do not present a higher barrier to entry or that larger deformations are already sampled by the protein. In addition, it is surprising that the entry rate is not slower than benzene since indole binds in a specific orientation in the cavity, while the benzene can rotate freely[23]. Apparently, the rate-limiting step for association does not involve 'freezing' out the indole's rotational freedom about the axis perpendicular to the ring plane. Either the fluctuations sampled by the protein are large enough to allow indole to change its entrance trajectory or indole reorients once in the cavity more rapidly than the rate limiting step.

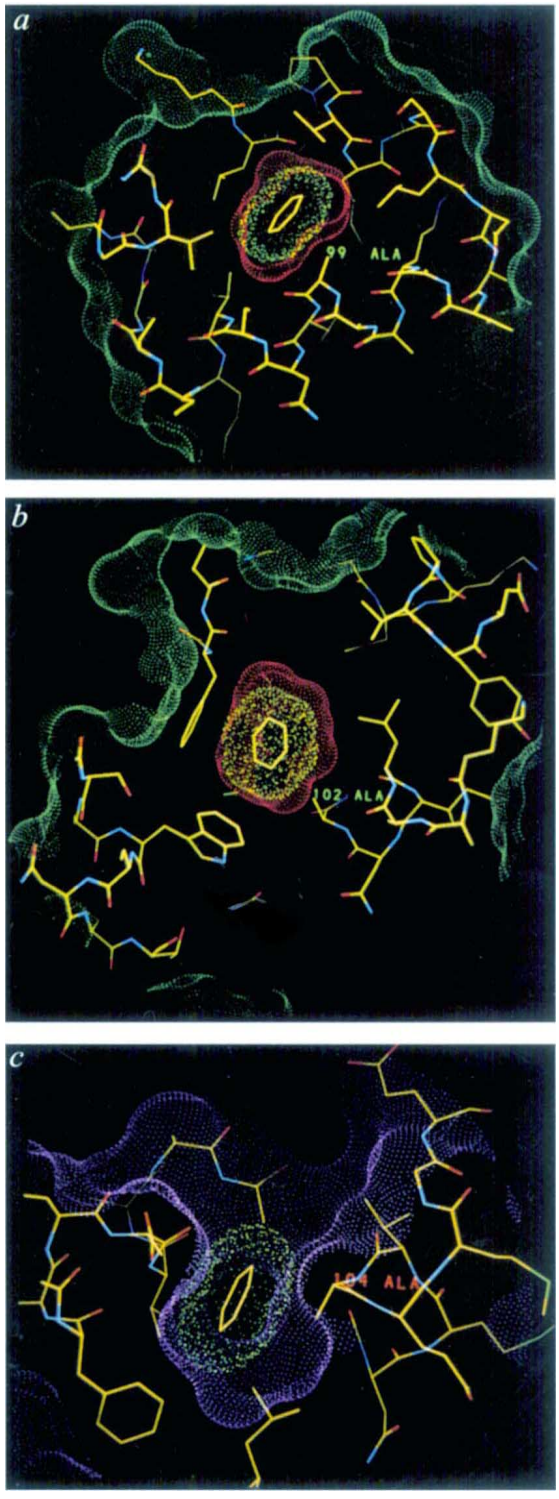

Low energy core deformations

The rapid entry of benzene and indole into buried cavities suggests that the required structural fluctuations are associated with small energetic changes. This conclusion is further supported by the relative temperature-independence of the association rate constants (Table 1). The faster rate of entry into Phe104Ala is presumably because the protein does not deform significantly (if at all) to create a path (Fig. 2*c*). By comparing association rate constants for the cavity and crevice variants and the diffusion-controlled encounter rates, we estimate an upper limit of 4–5 kcal mol^{-1} for the free energy barrier to entering the cavities[30]. Thus, structural changes large enough to allow benzene to enter the core have energetic obstacles comparable to rotations about one or two individual single bonds of butane[31]. The energetic barriers reported for the smaller Xe atom (2.05 Å radius) binding to buried sites in myoglobin are considerably larger (~16 kcal mol^{-1}; ref. 14). Although higher, this barrier does not suggest that large scale cooperative motions of the protein are likely needed for xenon access.

The apparent low activation energy for these deformations is similar to the apparent unfavourable reorganization energy incurred by substitutions of smaller residues for larger ones in a protein core (up to 5 kcal mol^{-1}; ref. 32). The accommodation of strain introduced by such mutations presumably reflects the static deformability of protein interiors. The dynamic flexibility we observe here may be further a expression of this static deformability.

Fig. 2 Benzene bound in cavities and cleft sites of T4 lysozyme variants. Crystallographic structures illustrate stippled Connolly surfaces of the cavities (red), cleft (purple) and protein surfaces (green) of the T4 lysozyme variants. The protein surface to cavity distances were estimated from Connolly surfaces[50] of the crystal structures to the benzene centre of mass. Connolly surfaces were generated using radii of Lee and Richards[51] and a probe size of 1.4 Å. The van der Waal surface of benzene is shown in yellow stippling. *a*, Leu99Ala–benzene, *b*, Met102Ala–benzene and c, Phe104Ala–benzene complexes (ref. 23, E.P.B. *et al.*, unpublished material). The surfaces are sectioned through the surface point closest to the benzene centre of mass.

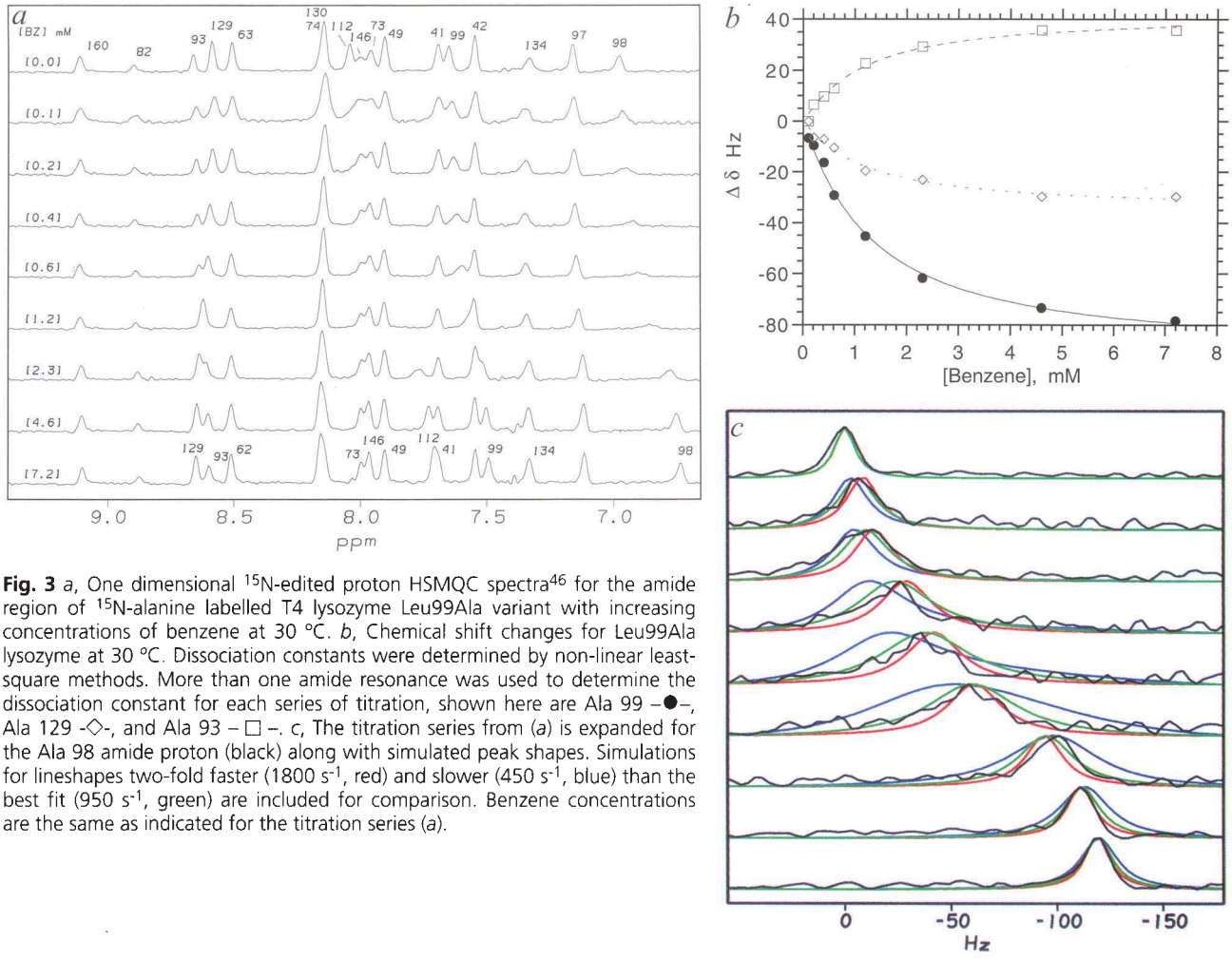

Fig. 3 *a*, One dimensional ^{15}N-edited proton HSMQC spectra[46] for the amide region of ^{15}N-alanine labelled T4 lysozyme Leu99Ala variant with increasing concentrations of benzene at 30 °C. *b*, Chemical shift changes for Leu99Ala lysozyme at 30 °C. Dissociation constants were determined by non-linear least-square methods. More than one amide resonance was used to determine the dissociation constant for each series of titration, shown here are Ala 99 –●–, Ala 129 -◇-, and Ala 93 – □ –. *c*, The titration series from (*a*) is expanded for the Ala 98 amide proton (black) along with simulated peak shapes. Simulations for lineshapes two-fold faster (1800 s^{-1}, red) and slower (450 s^{-1}, blue) than the best fit (950 s^{-1}, green) are included for comparison. Benzene concentrations are the same as indicated for the titration series (*a*).

Possible paths for entry

The path(s) and mechanism of the exchanging ligands remain(s) to be elucidated. Molecular dynamic simulations of CO and O_2 dissociation from the haem pocket of myoglobin suggest small fluctuations of buried side chains provide a path for escape[18]. It is possible that these proteins have evolved to provide such a path. Inspection of the T4 lysozyme structures suggests simple side-chain motions alone cannot generate a path: the cavities in the models remain inaccessible to a benzene-sized molecule even if all side chain atoms beyond Cβ are removed. The rate limiting steps may involve the ligand searching the protein surface for single or multiple entry site(s) and/or creating the entry path(s). The two closest surface points to the cavities which may be potential entry sites are adjacent to the most mobile helix in the C terminus, residues 108–113. This helix also has increased *B*-factors in the Leu99Ala–complex crystal structures compared to the apo structures[23,25], however similar increases in *B*-factors are not observed for the Met102Ala complex. The protein fluctuations necessary to create a path may occur by mobile defects or local unfolding of secondary structure[33–35]. These ligands could reduce the entry activation energy through favorable van der Waals interactions with atoms along the path.

'Polarity' barrier to protein permeability

These data have general implications for ligand binding dynamics in proteins. The rapid entry of these molecules into a protein core suggests that the ligand exchange rates from binding sites may not be strongly limited by either the steric barriers expected from examining crystal structures or the timescales of relatively large fluctuations. Entry may be limited by activation barriers resulting from the burial of dipoles or charges in the low dielectric protein interior and/or desolvation of polar groups. Thus, the general inability of polar molecules such as enzyme substrates to diffuse freely through proteins may be due to such 'polarity barriers' rather than steric occlusion.

The notion of a polarity barrier is also useful for understanding solvent exchange in proteins. Our data suggest that the observed slow exchange rate constants for some buried amide hydrogens (those amides defined as Peak 2 amides by Gregory and Lumry[36]) may be due to the unfavourable activation energy of transferring the exchanging species, a charged hydroxide ion or a water molecule, into the hydrophobic core instead of slow fluctuation rates necessary to create a free path (that is, the frequency of mobile defects[33,37] or so called steric gates[38]).

Generality to protein dynamics

The core of T4 lysozyme undergoes substantial deviations from its average structure and samples configurations with gaps between atoms large enough to admit a benzene or indole molecule on the timescale of milliseconds to microseconds. Are the types of deviations and the associated dynamic behaviour required for the permeability of benzene and indole generally available to all protein matrices? To address this question we need to understand whether the mutations that create the buried cavities significantly alter the dynamic nature of the core relative to wild type. Unfortunately, there is no published data that satisfactorily answers this question. Fast timescale dynamics can be affected by local core mutations: measurement of indole ring dynamics for a buried tryptophan suggest that the picosecond to nanosecond motions are increased when residues in van der Waal distance are altered[39]. Interestingly, such motions correlate more closely with the global stability of the protein rather than with local changes, that is, mutations that most affect the tryptophan dynamics on this timescale are far from the tryptophan and very destabilizing to the protein. The effects of changes in packing due to mutation in concerted motions on the millisecond to microsecond timescale range, those presumably required for ligand exchange, are also essentially unknown. One example of concerted fluctuations are those thought to be required for the ring flips observed for Tyr 35 and Phe 45 in bovine pancreatic trypsin inhibitor (BPTI). Ring flip rates for BPTI variants have been suggested to be governed by local packing rather than global stability, but the effects of adjacent residue substitutions have not investigated[40]. In our study, comparison of *B*-factors between the crystal structures of core variants and wild-type protein do not suggest changes in relative thermal motion as a consequence of the mutations. Rather the small differences observed are not localized to the mutation site and reflect the thermal factor differences between the data sets. The generality of the fluctuations described here are indicated by studies of ligand binding kinetics to myoglobin or hemoglobin[41–43] and the rate constants for CO, H_2S, and CS_2 quenching of tryptophan phosphorescence in azurin and alkaline phosphotase[21]. The rate constants for these data are similar for a number of proteins and processes which suggests that proteins may well be generally permeable to small molecules and invoke fluctuations on the millisecond to microsecond timescale.

Methods

Protein preparation and NMR conditions. Recombinant T4 lysozyme variants Leu99Ala[22], Met102Ala, and Phe104Ala in a Cys-free wt (wt*) background were generated according to methods described by M. Matsumura and B.W. Matthews[44]. Biosynthetic incorporation of ^{15}N-Ala into each T4 lysozyme variant was accomplished using published protocols[45]. Protein samples were dialyzed into 50 mM deuterated acetate buffer pH 5.5, concentrated to 0.3–0.4 mM, combined with ligand and sealed. Indole-containing samples were not sealed.

One dimensional ^{15}N-edited proton HSMQC spectra[46] were collected on a GN500 Omega spectrometer with spectral width 6666.7 Hz, 1024 points, 6400–9600 scans. All 17 alanine amide protons were observed for each variant. The ^{1}H,^{15}N HSMQC spectra for the ligand-free samples were compared to the T4 wt and wt* lysozyme assignments[47,48]. Comparison of the free and bound spectra showed only small changes for nitrogen chemical shift despite the large proton chemical shift changes for some of the resonances, facilitating assignment of the ligand bound proteins (data not shown).

The alanine amide resonances were divided into three types: Type 1 and Type 2 resonances correspond to the fast exchange regime and Type 3 resonances correspond to intermediate exchange regime on the NMR timescale. Those residues showing no change in chemical shift, Type 1 resonances, include the amides of alanine residues: 41, 42, 63, 97, 160 for all variants. Additionally, the alanine amide resonances of residues 49, 74, 130 for Leu99Ala, 49 and 93 for Met102Ala, and 74, 82, 93, and 130 for Phe104Ala were included as Type 1.

Determination of the equilibrium binding constant. For those resonances exhibiting fast exchange character and moderate chemical shift changes (Type 2), plots of chemical shift changes, $\Delta\delta$ (Hz), as a function of the total ligand concentration were fitted using the relationship, $\Delta\delta_{obs}=f_b\times\Delta\delta_{total}$ (where f_b is the fraction of ligand bound protein and $\Delta\delta_{total}$ is the total chemical shift change in Hz). The fraction bound is related to the dissociation constant, K_d (mM), and the ligand concentration, L (mM), by the relationship, $f_b = 1[(L)/(L+K_d)]$. The PlotData program (Triumph software) was used to estimate K_d and $\Delta\delta_{total}$ from the dependence of $\Delta\delta_{obs}$ as a function of total ligand concentration. The following Type 2 resonances were used to determine the equilibrium dissociation constants: Leu99Ala and benzene: 10 °C, 73 and 82; 20 and 30 °C, 93, 99 and 129; Met102Ala and benzene: 10 °C, 73, 129, 130 and 134; 20 °C ,74, 130 and 134; 30 °C 74 and 134; Phe104Ala and benzene: 7 °C, 104; 20°C, 49, 104; Leu99Ala and indole: 20 °C, 93, 97, 129.

Determination of rate constants. Lineshapes sensitive to uncoupled two-site exchange can be simulated from knowledge of k_{off}, f_b, $\Delta\delta_{total}$, T_{2f} ,and T_{2b} using modified Bloch equations derived by McConnell[27]. The observed lineshape is related to the sum of the population weighted lineshapes for free and bound protein ($1/T_{2f}$, $1/T_{2b}$) and the exchange rate constant, k_{ex}. At equilibrium, k_{ex} is related to the dissociation rate constant by $k_{ex}=k_{off}/f_b$. The f_b and $\Delta\delta_{total}$ values were estimated from calculated K_d values. Values for the transverse relaxation times for the free (T_{2f}) and bound (T_{2b}) protein were measured directly from spectral linewidths for free and ligand saturated protein, (linewidth at half-height for indole saturated Leu99Ala was equivalent to the ligand free protein). The assumption that the exchange process is two state is supported by a single ligand binding in each of the cavity/crevice containing variant crystal structures[23,25]. Each k_{off} rate constant (Table 1) was determined from comparison of observed peak shapes to a series of simulated titrations created over a range of possible off rate constants, 90–5000 s^{-1} at 50–100 s^{-1} intervals (Fig. 3*c*). The range of k_{off} rate constants in Table 1 were determined from the simulated titration curves which best fit not only the lineshape of the data (especially over the concentration range where the peak is most broadened) but also the relative position of the peak maxima as a function of concentration. Fig. 3*c* illustrates qualitatively that the rate constant is not slower than the values reported in Table 1. Further quantitative analysis using criterion described above provides certainty in the k_{off} rate constant within a twofold range or better. The simulations were generated by a program created by Michael Strain based on the approach of J. Sandström[49] and run as a macro by Felix version 2.05 software (Biosym Inc.). The following Type 3 resonances were used to calculate exchange rates: Leu99Ala and benzene: 10 °C, 93, 98, 112; 98 and 112 at 20 °C and 30 °C; Met102Ala and benzene: 10 °C, 134 only; 112 and 134 at 20 °C and 30 °C; Leu99Ala and indole: 98 and 112.

Estimates of the upper and lower k_{off} limits for the Phe104Ala benzene complex. The upper limit for the dissociation of benzene from the crevice, Phe104Ala, can be estimated using the conservative upper limit of k_{on}, 1×10^9 M^{-1} s^{-1} (refs 28, 29), the measured dissociation constant, 1×10^{-3} M, and the relationship $K_d k_{on}=k_{off}$. The lower limit was estimated by simulations to find the fastest k_{off} where line-broadening would not be observed, 10^4 s^{-1}. These estimates provide a k_{off} range of 10^4–10^6 s^{-1} for the Phe104Ala benzene complex.

Estimates of exchange rate by a global unfolding mechanism. The global unfolding rate can be estimated from the relationship K_{eq}=[folded]/[unfolded]=$k_{folding}/k_{unfolding}$. The equilibrium constant for Leu99Ala, ~10^7, was estimated from the wild-type K_{eq}, ~10^{10}, and the measured decrease in the T_m for Leu99Ala compared to wild type[23]. The folding rate constant measured for Leu99Ala in 50 mM sodium phosphate, 50 mM sodium chloride, pH 5.5 at 30 °C is 7 s^{-1} (ref. 48). These data provide an estimate of the apparent rate of unfolding, 10^{-7} s^{-1}, which is far too slow to account for the relatively fast k_{off} rate constants measured for benzene and indole.

Received 13 November 1995; accepted 17 April 1996.

Acknowledgements
The authors thank D. Barrick, M. Feese, J. Wray, N. Gassner, and B.W. Matthews for helpful discussions and comments on the manuscript. We also thank S. Snow and A. Roth for their technical assistance with protein preparation.

1. Miller, R.J.D. Energetics and dynamics of deterministic protein motion. *Accts. Chem. Res.* **27**, 145–150 (1994).
2. Karplus, M. & McCammon, J.A. The dynamics of proteins. *Sci. Amer.* April issue **4**, 42–51 (1986).
3. Debrunner, P.G. & Frauenfelder, H. Dynamics of proteins. *A. Rev. Phys. Chem.* **33**, 283–299 (1982).
4. Gurd, F.R.N. & Rothgeb, T.M. Motions in proteins. *Adv. Prot.Chem.* **33**, 73–165 (1979).
5. Karplus, M. & McCammon, J.A. Dynamics of proteins: elements and function. *A. Rev. Biochem.* **52**, 263–300 (1983).
6. Case, D.A. & Wright, P.E. Determination of high-resolution NMR structures of proteins, in *NMR of Proteins* (eds G.M. Clore & A.M. Gronenborn) 53–91 (MacMillian, London; 1993).
7. Smith, J.C. Protein dynamics: comparison of simulation with elastic neutron scattering experiments. *Q. Rev. Biophys.* **24**, 227–291 (1991).
8. McCammon, J.A., Lee, C.Y. & Northrup, S.H. Side-chain rotational isomerization in proteins: a mechanism involving gating and transient packing defects. *J. Am. Chem. Soc.* **105**, 2232–2237 (1983).
9. Kneller, G.R. & Smith, J.C. Liquid-like side-chain dynamics in myoglobin. *J. Mol. Bio.* **242**, 181–185 (1994).
10. Wagner, G. NMR relaxation and protein mobility. *Curr. Op. Struct. Biol.* **3**, 748–754 (1993).
11. Palmer III, A.G. Dynamic properties of proteins from NMR spectroscopy. *Curr. Op. Biotech.* **4**, 385–391 (1994).
12. Campbell, I.D., Dobson, C.M. & Williams, R.J.P. Proton magnetic resonance studies of the tyrosine residues of hen lysozyme - assignment and detection conformational mobility. *Proc. R. Soc. Lond. B.* **189**, 503–509 (1975).
13. Wüthrich, K. & Wagner, G. NMR investigations of the dynamics of the aromatic amino acid residues in the basic pancreatic trypsin inhibitor. *FEBS Lett.* **50**, 265–268 (1975).
14. Tilton, R.F. & Kuntz, I.D. Nuclear magnetic resonance studies of Xenon-129 with myoglobin and hemoglobin. *Biochemistry.* **21**, 6850–6857 (1982).
15. Tilton, R.F., Kuntz, I.D. & Petsko, G.A. Cavities in proteins: Structure of a metmyoglobin-xenon complex solved to 1.9 Å. *Biochemistry* **23**, 2849–2857 (1984).
16. Otting, G., Liepinsh, E. & Wüthrich, K. Proton exchange with internal water molecules in the protein BPTI in aqueous solution. *J. Am. Chem. Soc.* **113**, 4363–4364 (1991).
17. Otting, G. & Wüthrich, K. Studies of protein hydration in aqueous solution by direct NMR observation of individual protein-bound water molecules. *J. Am. Chem. Soc.* **111**, 1871–1875 (1989).
18. Elber, R. & Karplus, M. Enhanced sampling in molecular dynamics: use of the time dependent Hartree approximation for a simulation of carbon monoxide diffusion through myoglobin. *J. Am. Chem. Soc.* **112**, 9161–9175 (1990).
19. Brooks III, C.L., Karplus, M. & Pettitt, B.M. *Adv. in Chem. Phys.: Proteins: A Theoretical Perspective of Dynamics, Structure, and Thermodynamics* vol. 71 (eds I. Prigogine & S.A. Rice) 111–116 (John Wiley & Sons, New York; 1988).
20. Lakowicz, J.R. & Weber, G. Quenching of protein fluorescence by oxygen. Detection of structural fluctuations in proteins on the nanosecond timescale. *Biochemistry* **12**, 4171–4179 (1973).
21. Calhoun, D.B., Englander, S.W., Wright, W.W. & Vanderkooi, J.M. Quenching of room temperature protein phosphorescence by added small molecules. *Biochemistry* **27**, 8466–8474 (1988).
22. Eriksson, A.E. *et al.* Response of a protein structure to cavity-creating mutations and its relation to the hydrophobic effect. *Science* **255**, 178–183 (1992).
23. Eriksson, A.E., Baase, W.A., Wozniak, J.A. & Matthews, B.W. A cavity-containing mutant of T4 lysozyme is stabilized by a buried benzene. *Nature* **355**, 371–373 (1992).
24. Morton, A., Baase, W.A. & Matthews, B.W. Energetic origins of specificity of ligand binding in an interior nonpolar cavity of T4 lysozyme. *Biochemistry.* **34**, 8564–8575 (1995a).
25. Morton, A. & Matthews, B.W. Specificity of ligand binding in a buried nonpolar cavity of T4 lysozyme: linkage of dynamics and structural plasticity. *Biochemistry* **34**, 8576–8588 (1995).
26. Sangster, J. Octanol-water partition coefficients of simple organic compounds. *J. Phys. Chem. Ref. Data* **18**, 1111–1229 (1989).
27. McConnell, H.M. Reaction rates by nuclear magnetic resonance. *J. Chem. Phys.* **28**, 430–431 (1958).
28. Eigen, M. & Hammes, G.G. Elementary steps in enzyme reactions, in *Adv. in Enzym.* **25**, 1–38 (1963).
29. Fersht, A. In *Enzyme Structure and Mechanism, 2nd ed.* 150 (W. H. Freeman & Co., New York; 1985)
30. Berry, R.S., Rice, S.A. & Ross, J. In *Physical Chemistry* **30**, 1157–1164 (John Wiley & Sons, New York; 1980).
31. Streitwieser, A. & Heathcock, C.H. In *Introduction to Organic Chemistry, 3rd ed.* 70–72 (Macmillian, New York, 1985).
32. Baldwin, E.P. & Matthews, B.W. Core-packing constraints, hydrophobicity and protein design. *Curr. Op. in Biotech.* **5**, 396–402 (1994).
33. Lumry, R. & Rosenburg A. The water basis for mobile defects in proteins and the role of these defects in function. *Colloqu. Int. CNRS* **246**, 55–63 (1975).
34. Woodward, C., Simon, I. & Tuchsen, E. Hydrogen exchange and the dynamic structure of proteins. *Mol. Cell. Biochem.* **48**, 135–160 (1982).
35. Englander, S.W. & Kallenbach, N.R. Hydrogen exchange and structural dynamics of proteins and nucleic acids. *Quart. Rev. in Biophys.* **16**, 521–655 (1984).
36. Gregory, R. & Lumry R. Hydrogen exchange evidence for distinct structural classes in globular proteins. *Biopolymers* **24**, 301–326 (1985).
37. Richards, F. Packing defects, cavities, volume fluctuations and access to the interior of proteins. *Carlsberg Res. Commun.* **44**, 47–63 (1979).
38. Lumry, R. & Gregory, R.B. Free energy management in protein reactions: concepts, complications and compensation, in *The Fluctuating Enzyme* (ed. G.R Welch) 1–190 (John Wiley and Sons, New York; 1986).
39. Matthews, S.J., Jandu, S.K. & Leatherbarrow, R.J. ^{13}C NMR study of the effects of mutation on the tryptophan dynamics in chymotrypsin inhibitor 2: correlations with structure and stability. *Biochemistry* **32**, 657–662 (1993).
40. Wüthrich, K., Wagner, G., Richarz, R. & Braun, W. Correlations between internal mobility and stability of globular proteins. *Biophys. J.* **32**, 549–560 (1980).
41. Olsen, J.S., Mims, M.P. & Reisberg, P.I. Kinetic mechanisms of ligand binding to heme proteins in *Hemoglobin and Oxygen Binding* (C. Ho, ed.) 392–398 (Elsevier North Holland, Inc., New York; 1982).
42. Reisberg, P.I. & Olson, J.S. Rates of isonitrile binding to the isolated α and β subunits of human hemoglobin. *J. Biol. Chem.* **255**, 4151–4158 (1980).
43. Austin, R.H., Beeson, K.W., Eisenstein, L., Frauenfelder, H. & Gunsalus, I.C. Dynamics of ligand binding to myoglobin. *Biochemistry* **14**, 5355–5373 (1975).
44. Matsumura, M. & Matthews, B.W. Control of enzyme activity by an engineered disulfide bond. *Science* **243**, 792–794 (1989).
45. Muchmore, D.C., McIntosh, L.P., Russell, C.B., Anderson, D.E. & Dahlquist, F.W. Expression and nitrogen-15 labeling of proteins for proton and nitrogen-15 nuclear magnetic resonance. *Methods in Enzymology* **177**, 44–73 (1989).
46. Zuiderweg, E.R.B. A proton-detected heteronuclear chemical-shift correlation experiment with improved resolution and sensitivity. *J. Magn. Reson.* **86**, 346–357 (1990).
47. McIntosh, L.P., Wand, A.J., Lowry, D.F., Redfield, A.G. & Dahlquist, F.W. Assignment of the backbone ^1H and ^{15}N NMR resonances of bacteriophage T4 lysozyme. *Biochemistry* **29**, 6341–6362 (1990).
48. Lu, J. The Stability and Folding of Bacteriophage T4 Lysozyme. Doctoral Thesis, University of Oregon, 1992.
49. Sandström, J. In *Dynamic NMR Spectroscopy,* 6–19 (Academic Press, London; 1982).
50. Connolly, M.L. Solvent-accessible surfaces of proteins and nucleic acids. *Science* **221**, 709–713 (1983).
51. Lee, B.& Richards, F.M. The interpretation of protein structures: estimation of static accessibility. *J. Mol. Biol.* **55**, 379–400 (1971).